

Application News

UV-2600i UV-VIS Spectrophotometer, DUH™-210 Dynamic Ultra Micro Hardness Tester, AGX™-V Autograph Precision Universal Testing Machine, DSC-60 Plus Differential Scanning Calorimeter, IRTTracer™-100 Fourier Transform Infrared Spectrophotometer, SPM-Nanoa™ Scanning Probe Microscope/Atomic Force Microscope

Multifaceted Evaluation of Plastics: Differences due to PC/ABS Resin Compounding Ratio

Kazumi Kawahara, Fumiaki Yano, Tsukasa Nishimura, Masato Hirade, and Mitsuru Ohta

User Benefits

- ◆ Use of evaluation techniques that obtained linearity with respect to the material input ratio makes it possible to predict the compounding ratios of unknown materials.
- ◆ In comparison with a single control criterion, multifaceted evaluation is effective for reducing the risk of erroneous judgments.

Introduction

Polycarbonate (PC)/acrylonitrile-butadiene-styrene (ABS) resin is a thermoplastic resin with the added heat resistance and impact resistance of PC resin and the moldability and plating characteristics of ABS resin. Because of these properties, it is widely used in automotive interior parts, OA equipment, household electrical appliances, and various other products. Its properties can also be modified to meet various requirement specifications by changing the composition ratio of the PC/ABS resins. Since injection molding is complexly affected by multiple factors such as kneading, temperature, and pressure, the compounding ratio of materials input to the molding machine does not necessarily agree with the composition ratio after molding. For this reason, adjustment of the input compounding ratio during the production process to obtain the molded product with the intended composition ratio is extremely important. Here, the relationship between the compounding ratio and various properties was evaluated using five types of PC/ABS test specimens molded with different compounding ratios of PC and ABS (PC : ABS = 0 : 100, 25 : 75, 50 : 50, 75 : 25, 100 : 0). The agreement of the compounding ratios and the composition ratios after molding was also evaluated. In addition, scanning probe microscope (SPM) measurements were carried out for microscopic observation of the distribution of the component polymers.

Test Specimens

The test specimens were molded using a kneading machine and injection molding machine. Table 1 shows the kneading conditions, and Fig. 1 shows the appearance of the specimens.

Table 1 Kneading Conditions

PC:ABS	Kneading by kneading machine	Kneading by molding machine
0:100	None	220 °C • 250 s (approx.)
25:75	260 °C • 120 s (approx.)	260 °C • 250 s (approx.)
50:50	260 °C • 120 s (approx.)	260 °C • 250 s (approx.)
75:25	260 °C • 120 s (approx.)	260 °C • 250 s (approx.)
100:0	None	290 °C • 250 s (approx.)



Fig. 1 Appearance of Specimens
From left, PC : ABS = 0 : 100, 25 : 75, 50 : 50, 75 : 25, 100 : 0

Yellowness Index Measurement

When molded specimens are compared, their colors differ depending on the compounding ratio. Therefore, yellowness index was evaluated from UV-Vis absorption spectra obtained using a system combining an ultraviolet-visible spectrophotometer (UV) and an integrating sphere. Fig. 3 shows the reflection spectra of the test specimens.



Fig. 2 UV-2600i

Reflectance decreased as the ratio of ABS increased. Table 3 shows the yellowness index obtained from these results. It was found the yellowness index increases as the ABS compounding ratio increases.

Table 2 Measurement Conditions		Table 3 Results of Yellowness Index Measurements	
Instruments	: UV-2600i, ISR-2600Plus	PC:ABS	Yellowness
Measured wavelength range	: 380 - 780 nm	25:75	20.52
Data interval	: 1.0 nm	50:50	12.99
Scan speed	: Medium	75:25	8.48
Slit width	: 5.0 nm		

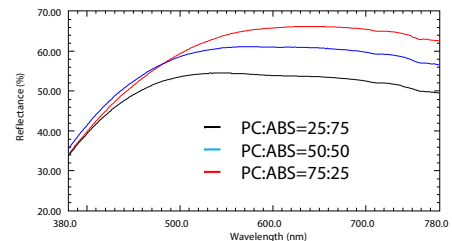


Fig. 3 Reflection Spectra of Specimens

Hardness Test

Next, the results of a hardness test using a dynamic ultra micro hardness tester (DUH) will be presented. As shown in Table 5, in the low PC ratio region, indentation hardness (HIT) showed a tendency to increase as the ratio of PC increased. However, the increase in HIT did not display linearity, as HIT showed its largest value at PC = 75 %, and was the same or slightly smaller than at 75 % when PC = 100 %.

Table 4 Measurement Conditions (Conforming to ISO/TS 19278)

Instrument	: DUH-210
Indenter	: Berkovich indenter
Test mode	: Load-unload test
Force	: 500 mN
Loading time/unloading time	: 30 s
Load holding time	: 40 s
Number of tests	: 5 (central 3 tests were extracted)
Ambient temperature	: 23±2 °C
Humidity	: 50±10 %

Table 5 Test Results

PC:ABS	HIT (MPa)
0:100	156.1
25:75	159.6
50:50	164.3
75:25	170.8
100:0	169.9



Fig. 4 DUH™-210

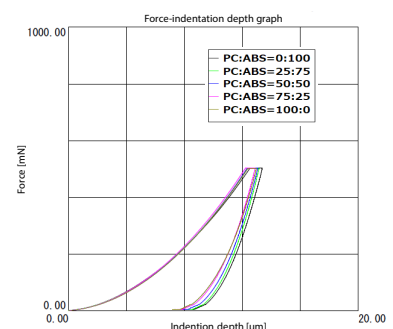


Fig. 5 Test Curves

Tensile Test

A tensile test was conducted using a precision universal testing machine. In this test, a noncontact type TRViewX extensometer was used as the extensometer. Fig. 7 shows the condition of the test, and Fig. 8 shows representative graphs of specimens with the various compounding ratios. Figs. 9 to 11 show the tensile strength, elastic modulus, and breaking elongation, respectively, for the various compounding ratios. Tensile strength and breaking elongation increased as the compounding ratio of PC increased. However, the elastic modulus showed its largest values at the PC ratios of 50 to 75 %. In Fig. 12, approximate linearity of the plots of tensile strength against the compounding ratio of PC was confirmed, suggesting that the compounding ratio can be predicted from tensile strength.



Fig. 6 AGX™-V



Fig. 7 Condition of Tensile Test

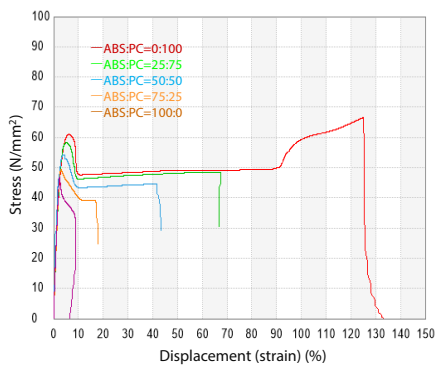


Fig. 8 Test Curves

Table 6 Instrument Configuration and Test Conditions

Precision universal testing: AGX-V machine	
Load cell	: 5 kN
Grip	: Pneumatic flat grip
Extensometer	: TRViewX240S
Software	: TRAPEZIUM™X-V
Test speed	: 1 mm/min 50 mm/min (switched at displacement of 0.3 %)
Gauge length	: 75 mm
Number of tests	: n=5
Specimen width	: 10 mm
Specimen thickness	: 4 mm
Grip distance	: 115 mm

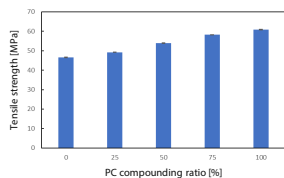


Fig. 9 Tensile Strength

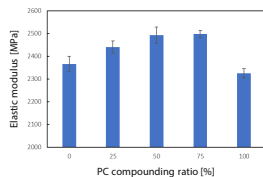


Fig. 10 Elastic modulus

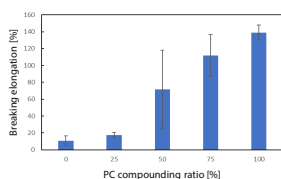


Fig. 11 Breaking elongation

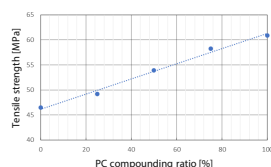


Fig. 12 Relationship between Tensile Strength and Compounding Ratio

Thermal Analysis

Next, this section presents the results of measurements using a differential scanning calorimeter (DSC). Fig. 14 shows the DSC curves. Two changes could be seen at the glass transition points of ABS (Tg1) and PC (Tg2). Fig. 15 shows the relationship between the glass transition points and the compounding ratio of PC. Since linearity was obtained in the relationships between the two, it was suggested that the compounding ratio can be predicted from the glass transition point.



Fig. 13 DSC-60Plus

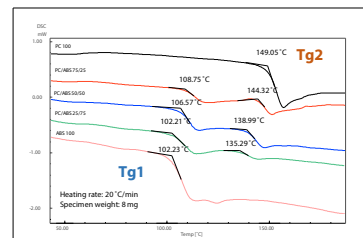


Fig. 14 DSC Curves

Table 7 Measurement Conditions

Instrument	: DSC-60 Plus
Heating rate	: 20 °C/min
Specimen weight	: 8 mg
Atmosphere	: Nitrogen

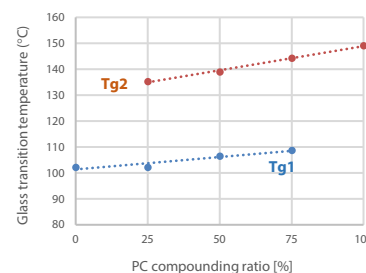


Fig. 15 Relationship between PC Compounding Ratio and Glass Transition Points

Composition Analysis

This section shows the results of composition measurements using a Fourier transform infrared spectrophotometer (FTIR). Figs. 17 and 18 show the infrared spectra of each specimen and the relationship between the PC compounding ratio and peak intensity, respectively. The peak intensity (1770 cm⁻¹) of the C=O bond originating from PC increased in proportion to the PC compounding ratio. As high linearity was obtained between the two, agreement of the compounding ratio and the composition ratio after molding was confirmed.



Fig. 16 IRTracer™-100

Table 8 Measurement Conditions

Instrument	: IRTracer-100, QATR™10 (diamond prism)
Wavelength range	: 400 - 4000 cm ⁻¹
Resolution	: 4 cm ⁻¹
Accumulation	: 40 times
Apodization function	: Happ-Genzel
Detector	: DLATGS

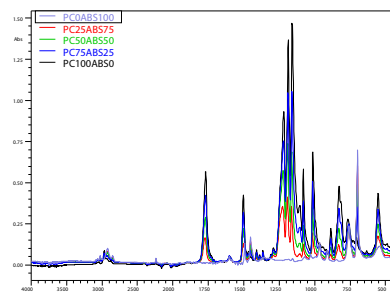


Fig. 17 Infrared Spectra of Specimens

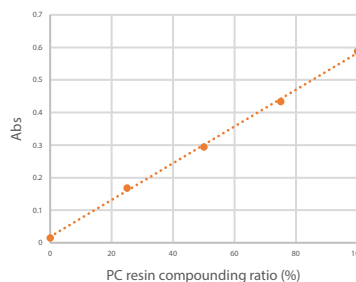


Fig. 18 Relationship between PC Compounding Ratio and Peak Intensity

Microscopic Observation

In blended polymers, the state of distribution of the constituent polymers is assumed to affect the strength of the material, and an understanding of this relationship is also important for molding. Here, images of the hardness distribution of the surface were obtained by using a scanning probe microscope/atomic force microscope (SPM) utilizing Nano 3D Mapping Fast, which is one measurement mode of the SPM, for three specimens with the compounding ratios of PC : ABS = 0 : 100, 25 : 75, and 100 : 0. Fig. 20 to Fig. 23 show the results of an evaluation of the distribution states of the polymers. In these images, lighter colors indicate harder materials.

In the image of the compounding ratio of PC : ABS = 0 : 100 in Fig. 20, the rubber component is distributed in an island-like form in a matrix phase (relatively lighter colored part) consisting of an acrylonitrile-styrene copolymer. Conversely, at the compounding ratio of PC : ABS = 100 : 0 in Fig. 21, only the PC phase can be observed. At the compounding ratio of PC : ABS = 25 : 75 in Fig. 22, mainly three phases can be observed, and that with the lightest color is considered to be PC phase. In Fig. 23, these PC regions are represented by yellow. The ratio occupied by the yellow parts in the total image is approximately 25%, which agrees with the compounding ratio of PC, and the PC is also distributed uniformly.



Fig. 19 SPM-Nanoa™

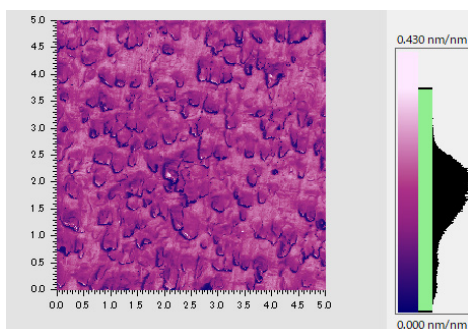


Fig. 20 PC : ABS = 0 : 100

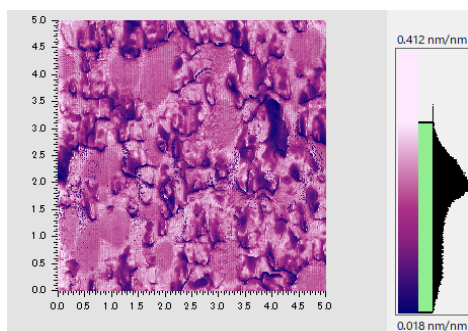


Fig. 22 PC : ABS = 25 : 75

Conclusion

In these experiments, it was possible to confirm the relationship between various material properties and the compounding ratio of a blended polymer by multifaceted measurements of PC/ABS specimens molded with different compounding ratios.

UV measurement confirmed that yellowness increases when the ABS compounding ratio is increased.

Since it was possible to confirm agreement of the compounding ratios of the materials charged into the molding machine and the composition ratios of the specimens after molding by a quantitative evaluation utilizing FTIR, and linearity was obtained between the composition ratios of the specimens after molding and the tensile strength measured with a tensile tester and the glass transition points measured by DSC, these evaluation methods are considered to be effective means for simple confirmation of the composition ratios of molded products. Based on the results of evaluations of the composition ratios of the specimens after molding by FTIR and the measurements of physical properties by tensile testing and thermal analysis, it was suggested that multifaceted evaluation can enhance the reliability of quality control while also improving work efficiency by simple measurement techniques.

On the other hand, in the measurement results, linearity of the elastic modulus and indentation hardness with respect to the compounding ratio could not be obtained. The reason for this is still unclear, but we conjecture that other factors, in addition to the compounding ratio, are affecting the measurement results. There is a possibility that the distribution condition of the polymers measured by SPM in this experiment may affect changes in strength properties such as the elastic modulus. Thus, a detailed analysis of the relationship between the microscopic structure and the strength properties of blended polymers with different compounding ratios is considered to be the next issue for study.

Table 9 Measurement Conditions

Instrument	: SPM-Nanoa
Measurement mode	: Nano 3D Mapping Fast
Observation field	: 5 μm × 5 μm

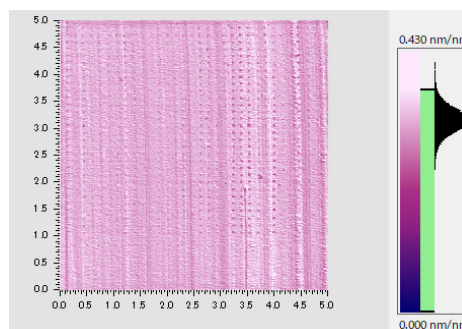


Fig. 21 PC : ABS = 100 : 0

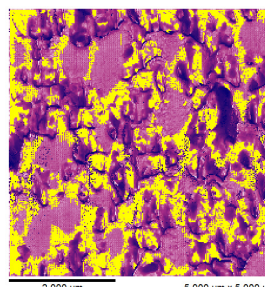


Fig. 23 Distribution of PC Phase

DUH, AGX, TRAPEZIUM, IRTTracer, and SPM-Nanoa are trademarks of Shimadzu Corporation or its affiliated companies in Japan and/or other countries.



Shimadzu Corporation

www.shimadzu.com/an/

For Research Use Only. Not for use in diagnostic procedures.

This publication may contain references to products that are not available in your country. Please contact us to check the availability of these products in your country.

The content of this publication shall not be reproduced, altered or sold for any commercial purpose without the written approval of Shimadzu. See <http://www.shimadzu.com/about/trademarks/index.html> for details.

Third party trademarks and trade names may be used in this publication to refer to either the entities or their products/services, whether or not they are used with trademark symbol "TM" or "®".

Shimadzu disclaims any proprietary interest in trademarks and trade names other than its own.

The information contained herein is provided to you "as is" without warranty of any kind including without limitation warranties as to its accuracy or completeness. Shimadzu does not assume any responsibility or liability for any damage, whether direct or indirect, relating to the use of this publication. This publication is based upon the information available to Shimadzu on or before the date of publication, and subject to change without notice.

01-00588-EN

First Edition: Oct. 2023